

Electronic Supplementary Information

Development of NMR and thermal shift assays for the evaluation of *Mycobacterium tuberculosis* isocitrate lyase inhibitors

Ram Prasad Bhusal,¹ Krunal Patel,¹ Brooke X. C. Kwai,^{1,†} Anne Swartjes,^{1,†} Ghader Bashiri,^{2,3}

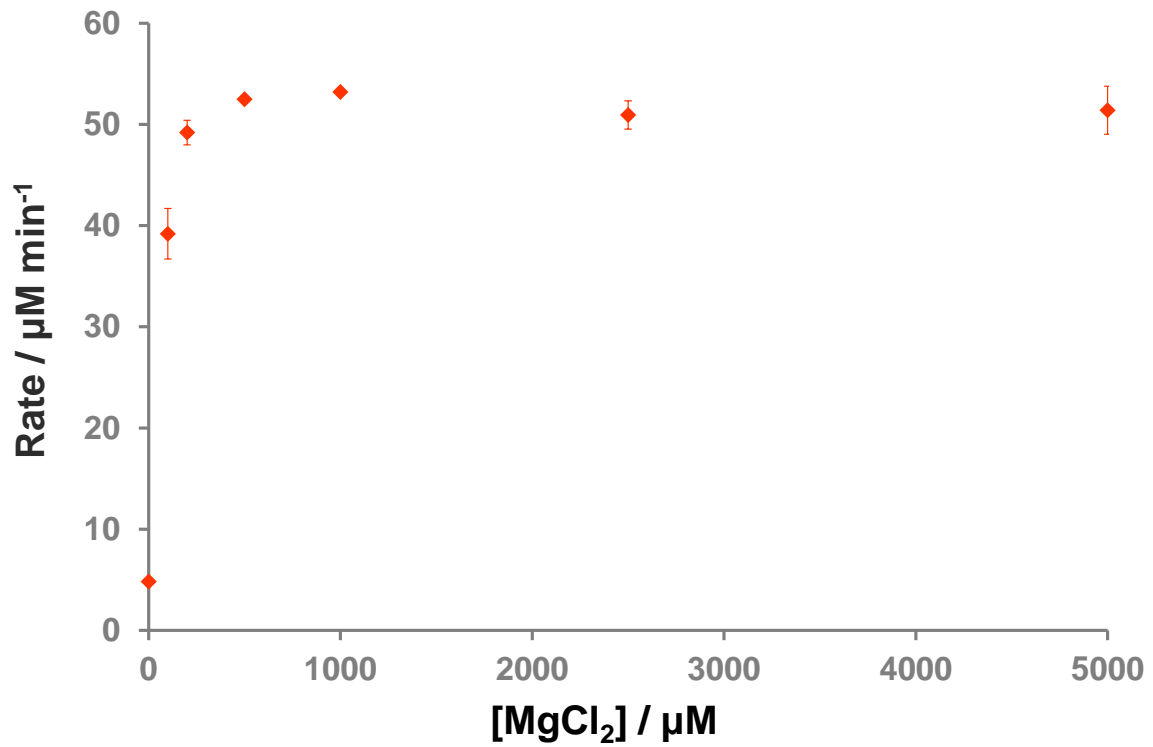
Jóhannes Reynisson,¹ Jonathan Sperry*,¹ and Ivanhoe K. H. Leung*,¹

1. School of Chemical Sciences, The University of Auckland, Private Bag 92019, Victoria Street West, Auckland 1142, New Zealand.

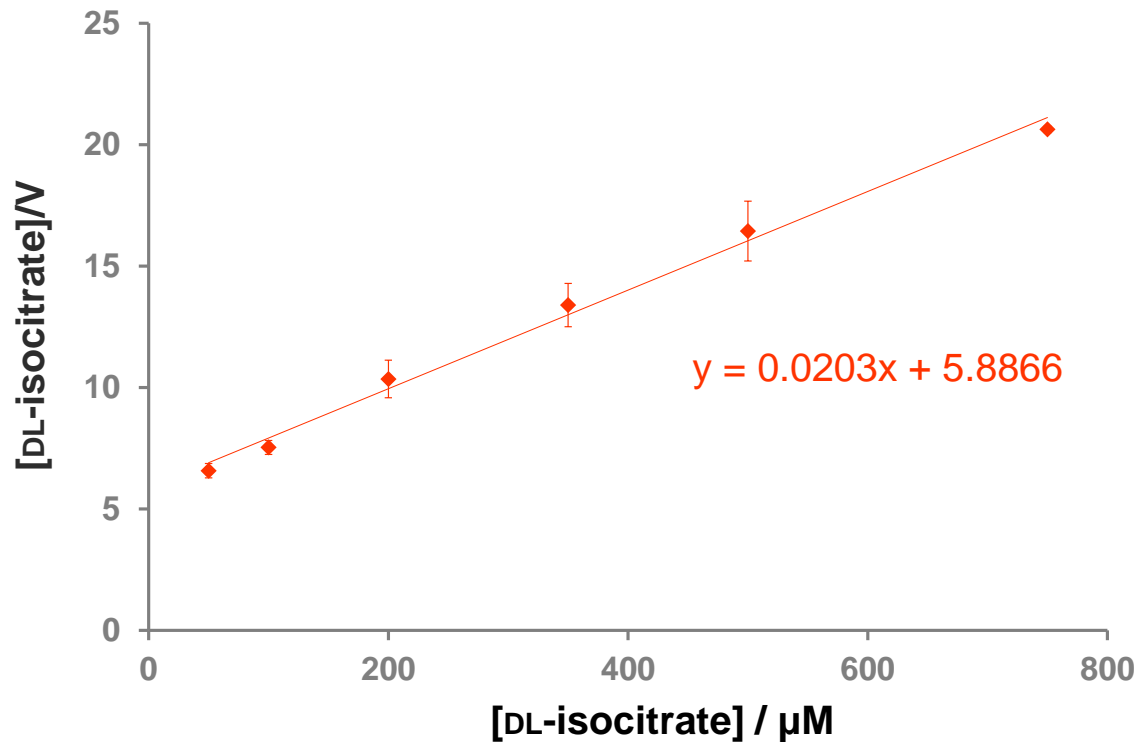
2. School of Biological Sciences, The University of Auckland, Private Bag 92019, Victoria Street West, Auckland 1142, New Zealand.

3. Maurice Wilkins Centre for Molecular Biodiscovery, The University of Auckland, Private Bag 92019, Victoria Street West, Auckland 1142, New Zealand.

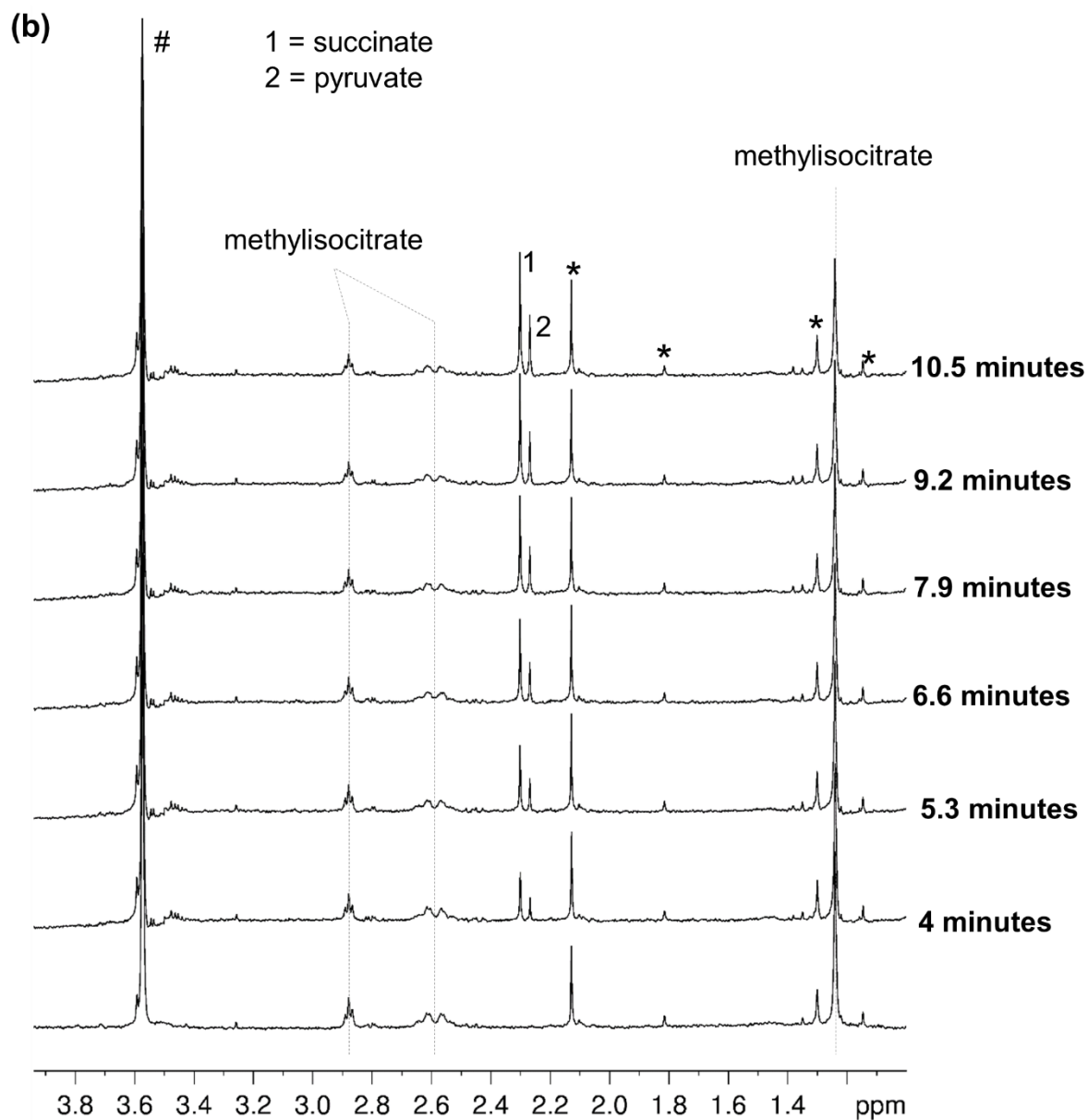
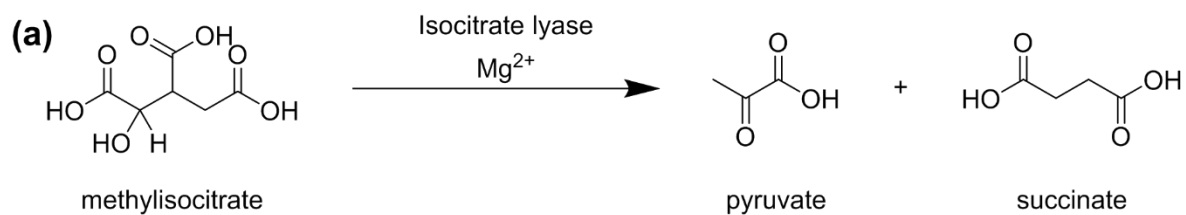
† These authors contributed equally to this work.



Supplementary Figure S1: Mg²⁺ is required for optimal ICL1 activity. Sample contained 190 nM ICL1, 1 mM DL-isocitrate, varying concentration of MgCl₂ and 50 mM Tris/Tris-D₁₁ (pH 7.5) in 90% H₂O and 10% D₂O. The errors shown are the standard deviation from three separate measurements.

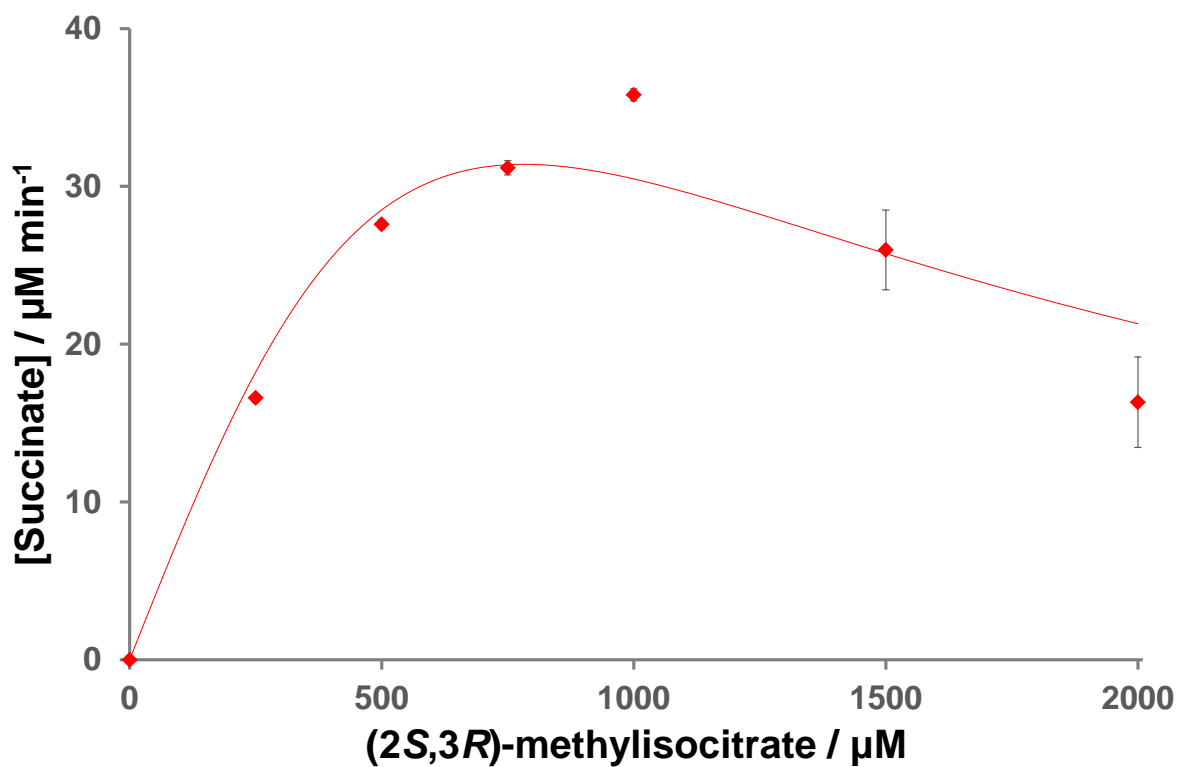


Supplementary Figure S2: Hanes plot of ICL1. Sample contained 190 nM ICL1, varying concentration of DL-isocitrate, 5 mM MgCl_2 and 50 mM Tris/Tris- D_{11} (pH 7.5) in 90% H_2O and 10% D_2O . The errors shown are the standard deviation from three separate measurements. The Michaelis constant (K_M) was found to be $290 \pm 10 \mu\text{M}$ and the catalytic constant (k_{cat}) was found to be $4.3 \pm 0.1 \text{ s}^{-1}$.

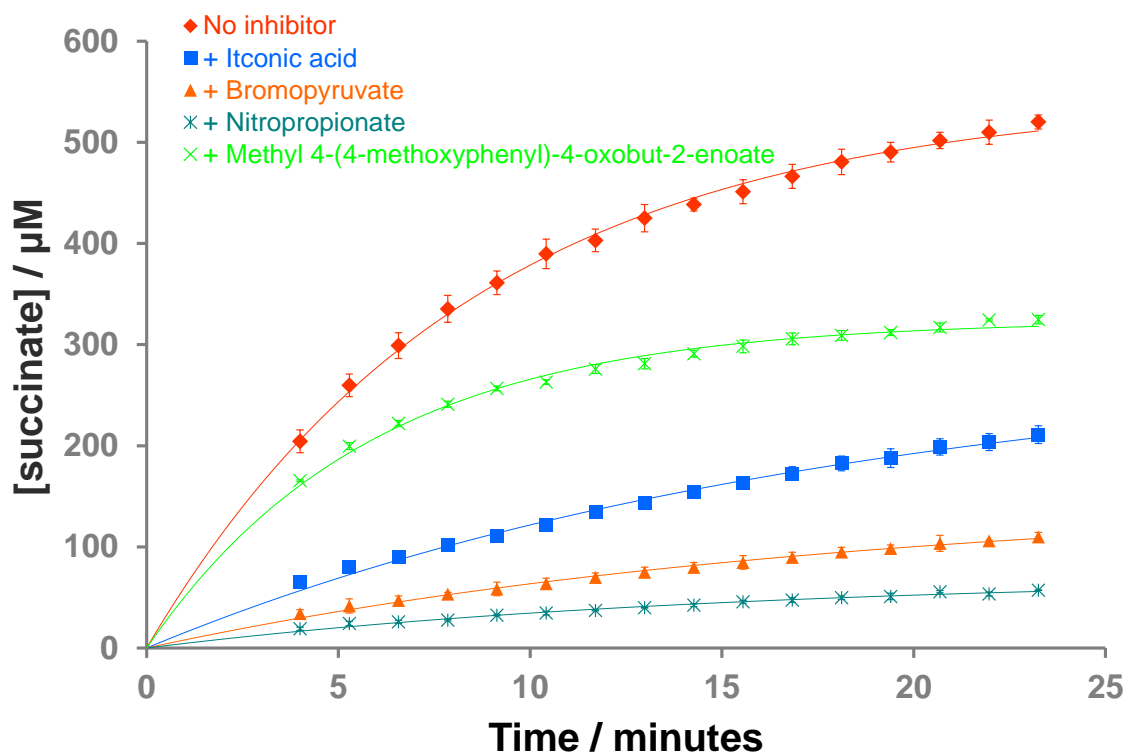


Supplementary Figure S3: (a) Isocitrate lyase catalyses the conversion of methylisocitrate to pyruvate and succinate; (b) ^1H NMR spectroscopy to monitor ICL1-catalysed turnover of (2*S*,3*R*)-2-methylisocitrate into pyruvate and succinate. Sample contained 190 nM ICL1, 1 mM (2*S*,3*R*)-2-methylisocitrate, 5 mM MgCl_2 and 50 mM Tris/Tris- D_{11} (pH 7.5) in 90% H_2O and

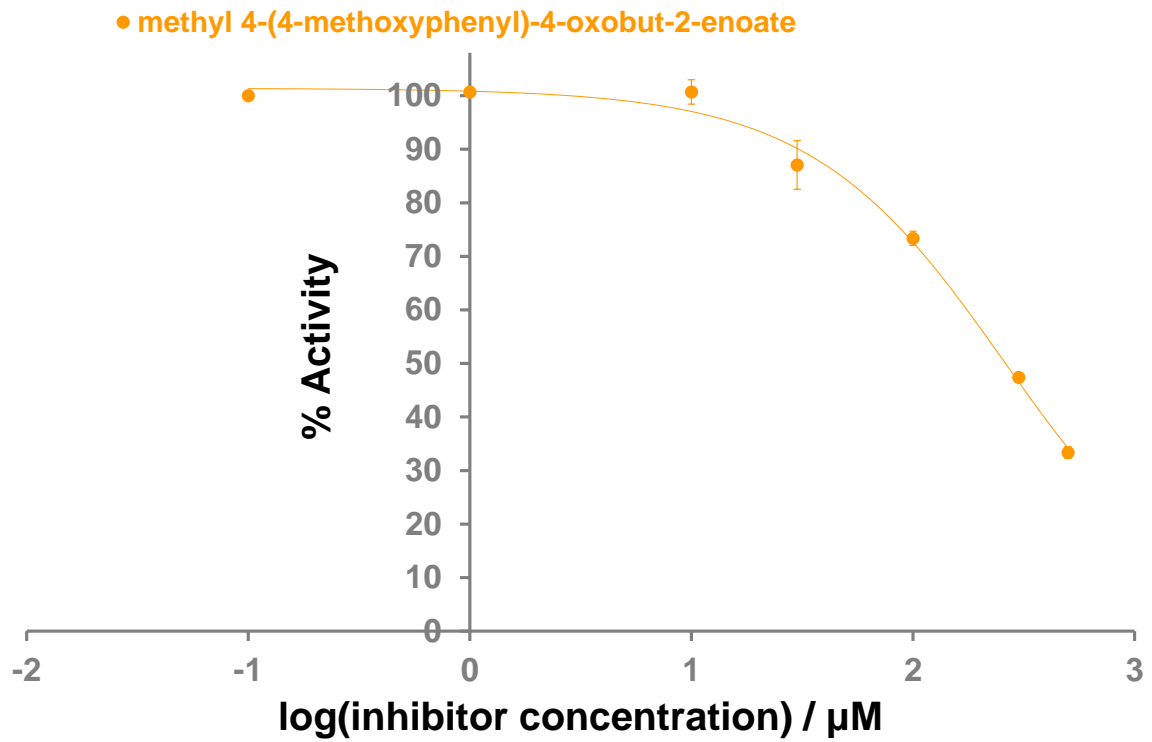
10% D₂O. The hashtag (#) indicates Tris/Tris-D₁₁ peak. Asterisks (*) indicate impurities from buffer and/or methylisocitrate stock solution.



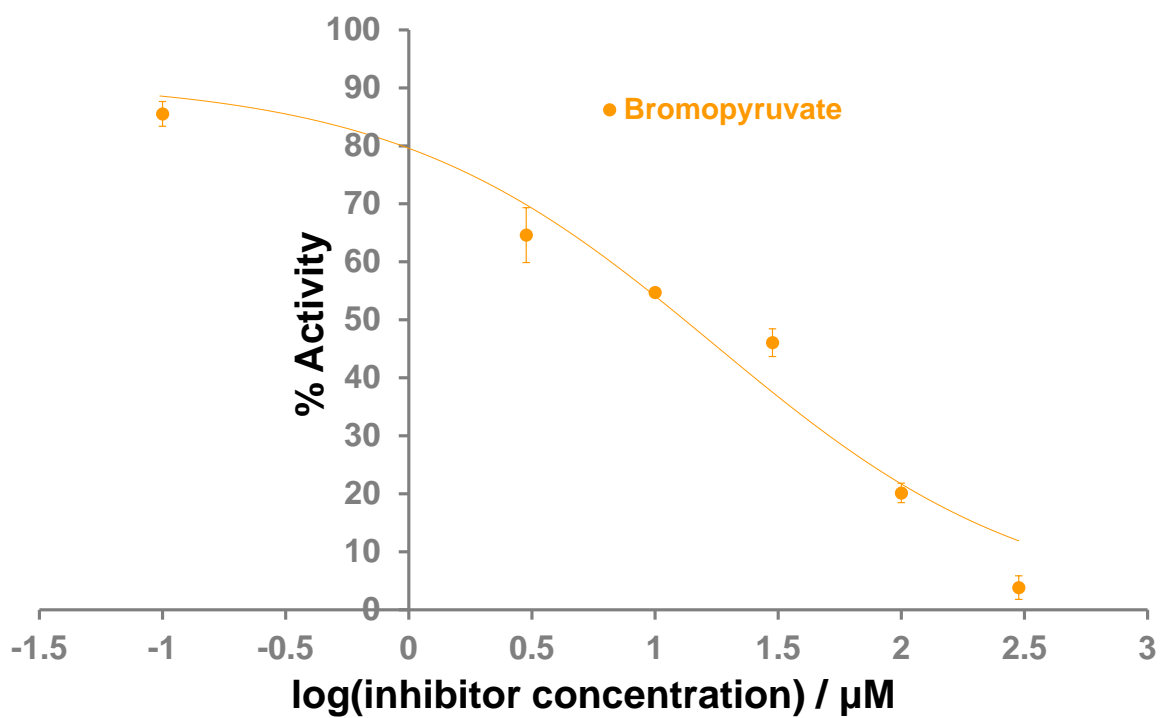
Supplementary Figure S4: Substrate inhibition was observed when (2*S*,3*R*)-2-methylisocitrate was used as substrate. The curve was added to aid visualisation. Sample contained 190 nM ICL1, 1 mM (2*S*,3*R*)-2-methylisocitrate, 5 mM MgCl₂ and 50 mM Tris/Tris-D₁₁ (pH 7.5) in 90% H₂O and 10% D₂O. The errors shown are the standard deviation from three separate measurements.



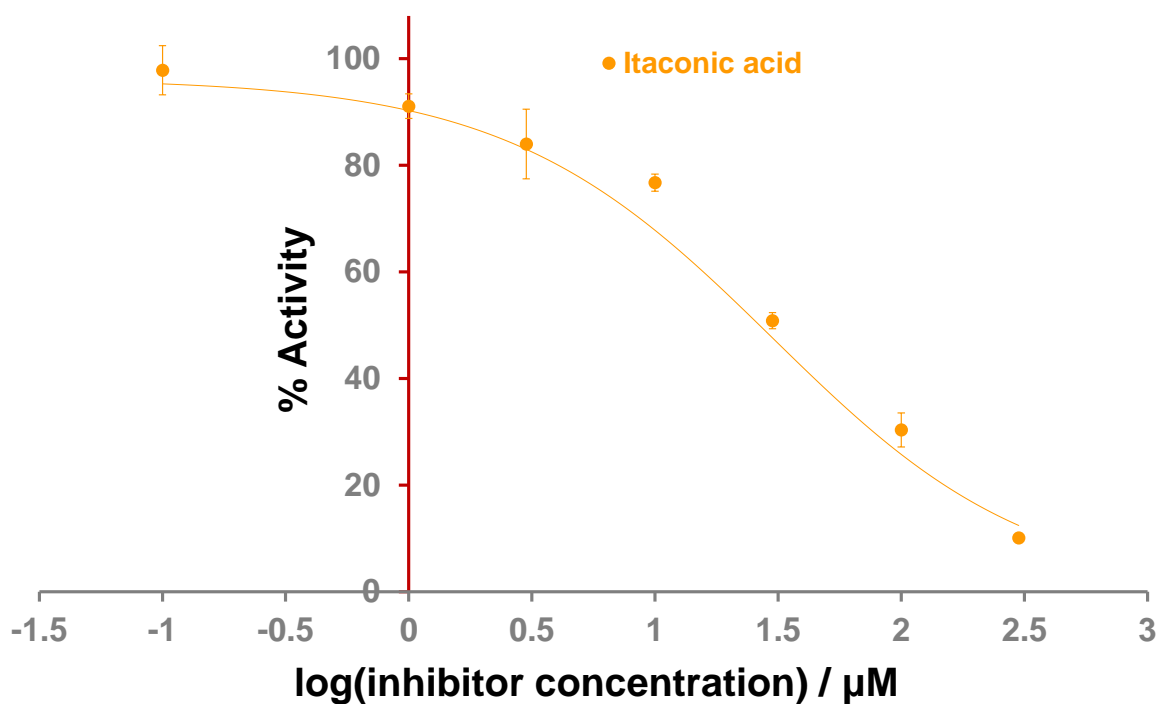
Supplementary Figure S5: Single concentration inhibition data of ICL1 inhibitors. Sample contained 190 nM ICL1, 1 mM DL-isocitrate, 100 μM inhibitor (if applicable), 5 mM MgCl₂ and 50 mM Tris/Tris-D₁₁ (pH 7.5) in 90% H₂O and 10% D₂O. The curves were added to aid visualisation. The errors shown are the standard deviation from three separate measurements.



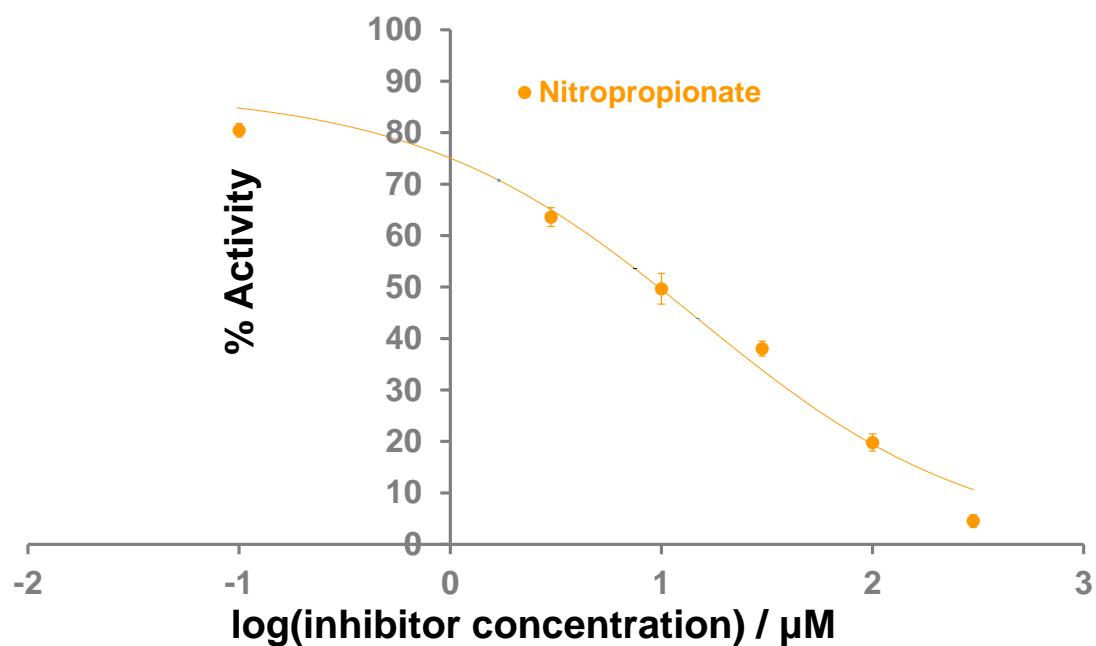
Supplementary Figure S6: IC_{50} measurement for methyl 4-(4-methoxyphenyl)-4-oxobut-2-enoate). Samples contained 190 nM ICL1, 1 mM DL-isocitrate, varying concentration of inhibitor, 5 mM MgCl_2 and 50 mM Tris/Tris- D_{11} (pH 7.5) in 90% H_2O and 10% D_2O . The errors shown are the standard deviation from three separate measurements. IC_{50} was 250 ± 7 μM .



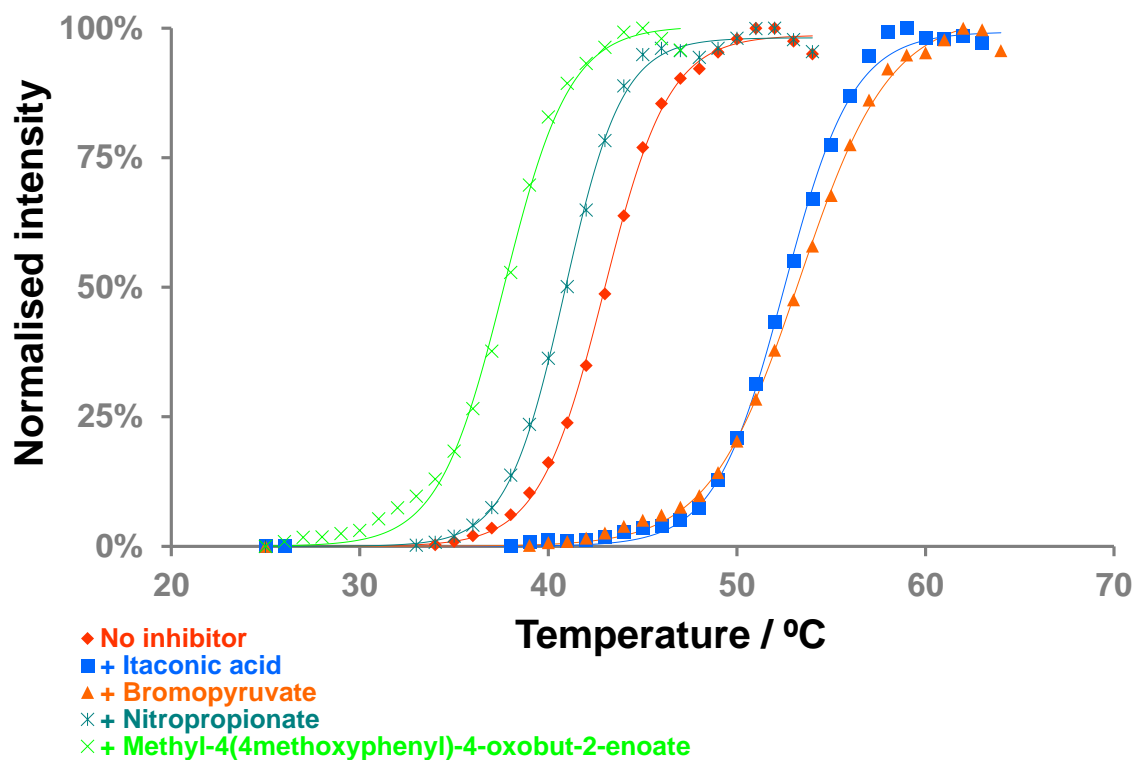
Supplementary Figure S7: IC₅₀ measurement for bromopyruvate. Samples contained 190 nM ICL1, 1 mM DL-isocitrate, varying concentration of inhibitor, 5 mM MgCl₂ and 50 mM Tris/Tris-D₁₁ (pH 7.5) in 90% H₂O and 10% D₂O. The errors shown are the standard deviation from three separate measurements. IC₅₀ was 17.5 ± 1.0 μM.



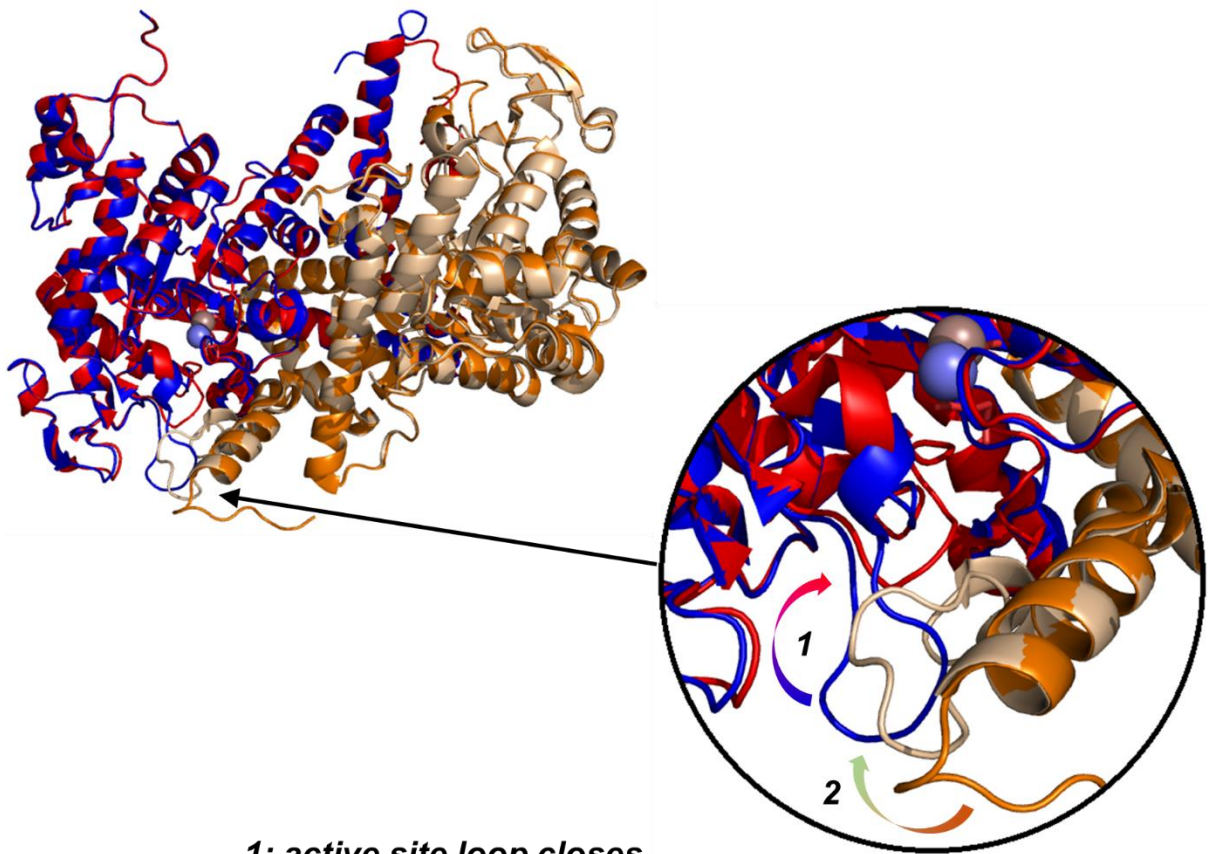
Supplementary Figure S8: IC₅₀ measurement for itaconic acid. Samples contained 190 nM ICL1, 1 mM DL-isocitrate, varying concentration of inhibitor, 5 mM MgCl₂ and 50 mM Tris/Tris-D₁₁ (pH 7.5) in 90% H₂O and 10% D₂O. The errors shown are the standard deviation from three separate measurements. IC₅₀ was 29.4 ± 4.1 μM.



Supplementary Figure S9: IC₅₀ measurement for nitropropionate. Samples contained 190 nM ICL1, 1 mM DL-isocitrate, varying concentration of inhibitor, 5 mM MgCl₂ and 50 mM Tris/Tris-D₁₁ (pH 7.5) in 90% H₂O and 10% D₂O. The errors shown are the standard deviation from three separate measurements. IC₅₀ was 14.7 ± 1.8 μM.



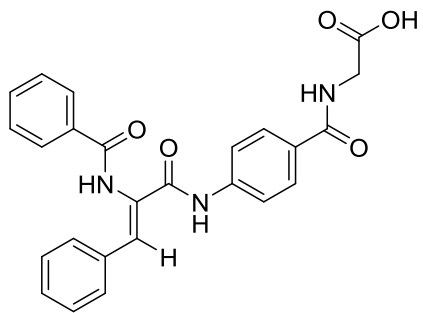
Supplementary Figure S10: Protein melt curve for ICL1 inhibitors. Sample contained 20 μM ICL1, 1 mM compounds (where applicable) and 1 mM MgCl_2 in 50 mM Tris-HCl pH 7.5. Temperature was increased from 25 to 95 $^{\circ}\text{C}$ at 1 $^{\circ}\text{C}$ increment every 60 seconds. The melting temperature of ICL1 in the presence of MgCl_2 was 43.0 $^{\circ}\text{C}$. The melting temperatures of ICL1 in the presence of 3-bromopyruvate, itaconic acid, 3-nitropropionate and methyl 4-(4-methoxyphenyl)-4-oxobut-2-enoate were 52.5 $^{\circ}\text{C}$, 53.3 $^{\circ}\text{C}$, 40.9 $^{\circ}\text{C}$ and 37.6 $^{\circ}\text{C}$ respectively.



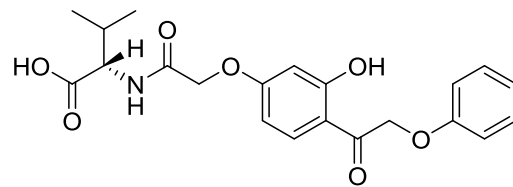
1: active site loop closes
**2: C-terminal of the adjacent subunit moves over
and interacts with the closed loop**

Supplementary Figure S11: A two-step conformational change was observed when ICL1 was bound to glyoxylate and nitropropionate (PDB ID: 1F8I; subunit A: red; subunit B: wheat; only two subunits shown) when compared to the crystal structure of *apo*-ICL1 (PDB id: 1f61; crystallised as a dimer; subunit A: blue and subunit B: orange).

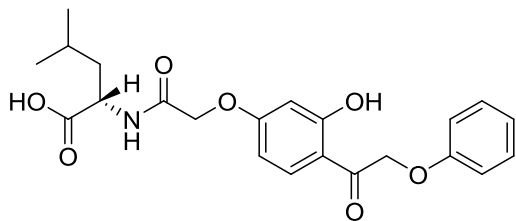
1



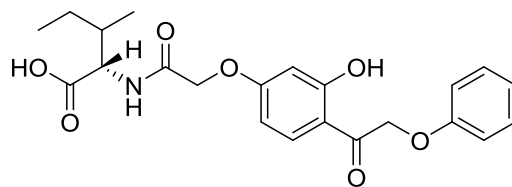
2



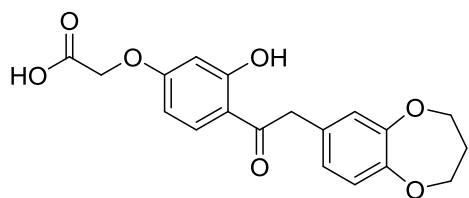
3



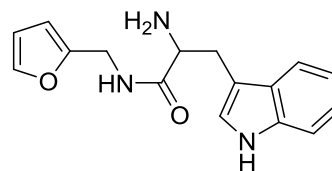
4



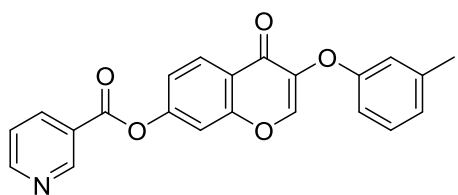
5



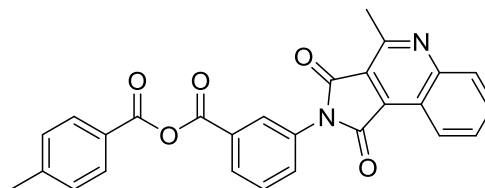
6



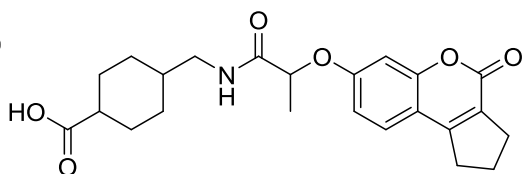
7



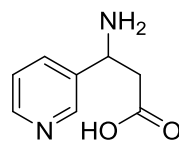
8



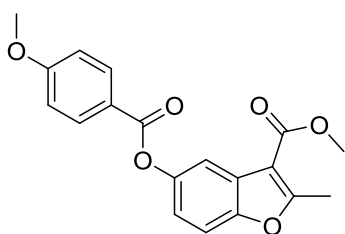
9



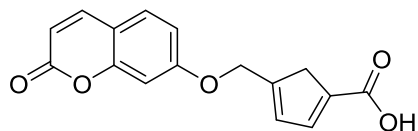
10

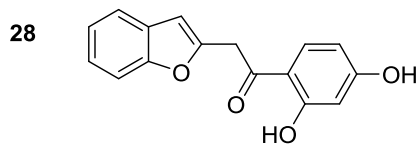
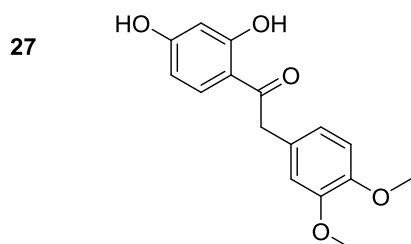
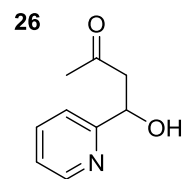
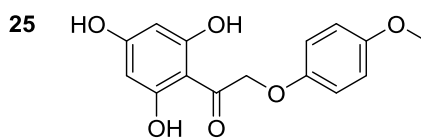
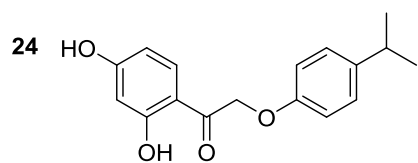
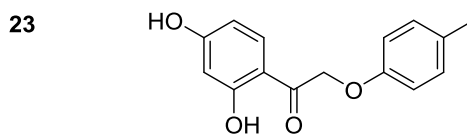
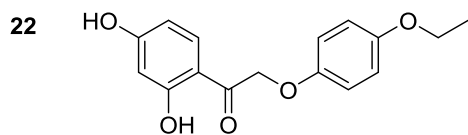
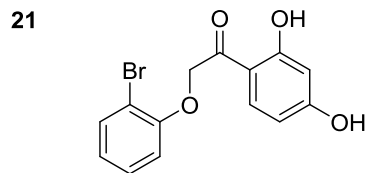
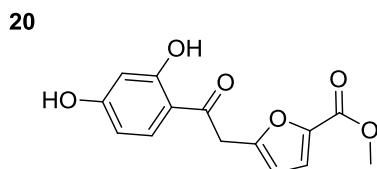
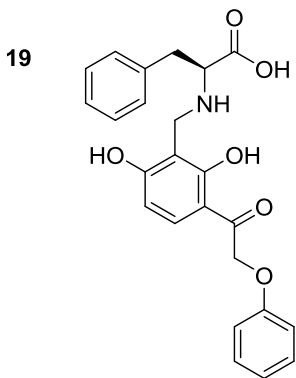
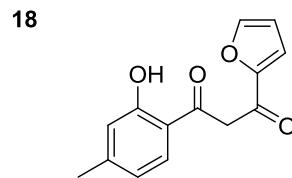
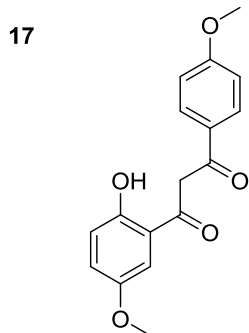
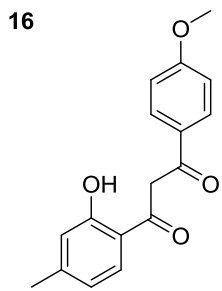
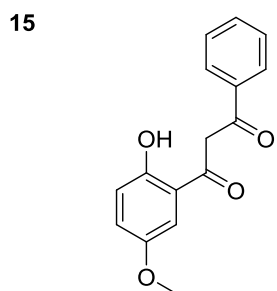
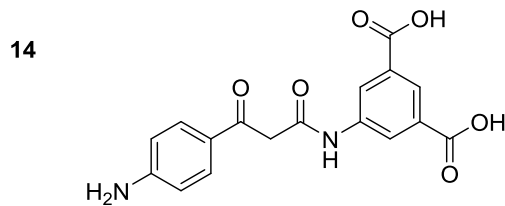
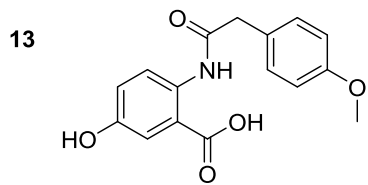


11

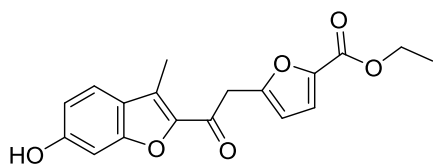


12

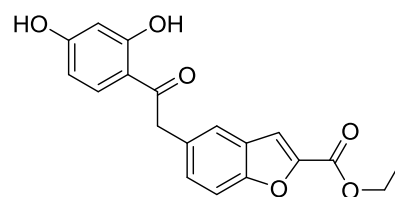




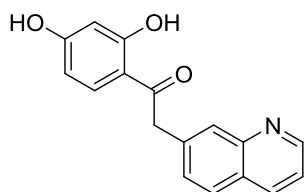
29



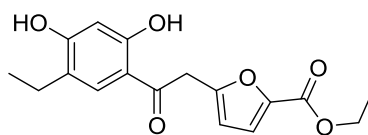
30



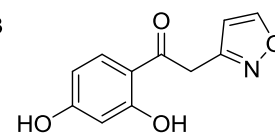
31



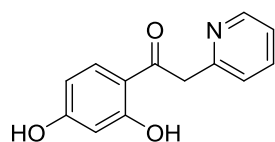
32



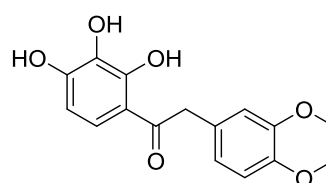
33



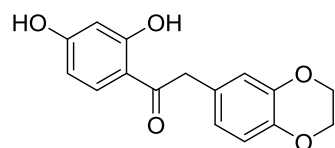
34



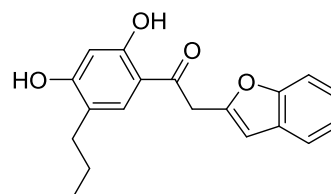
35



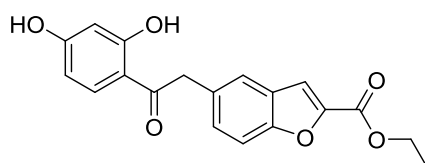
36



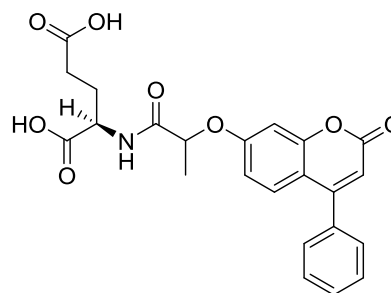
37



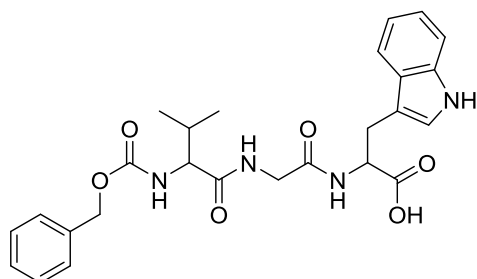
38



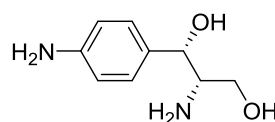
39



40

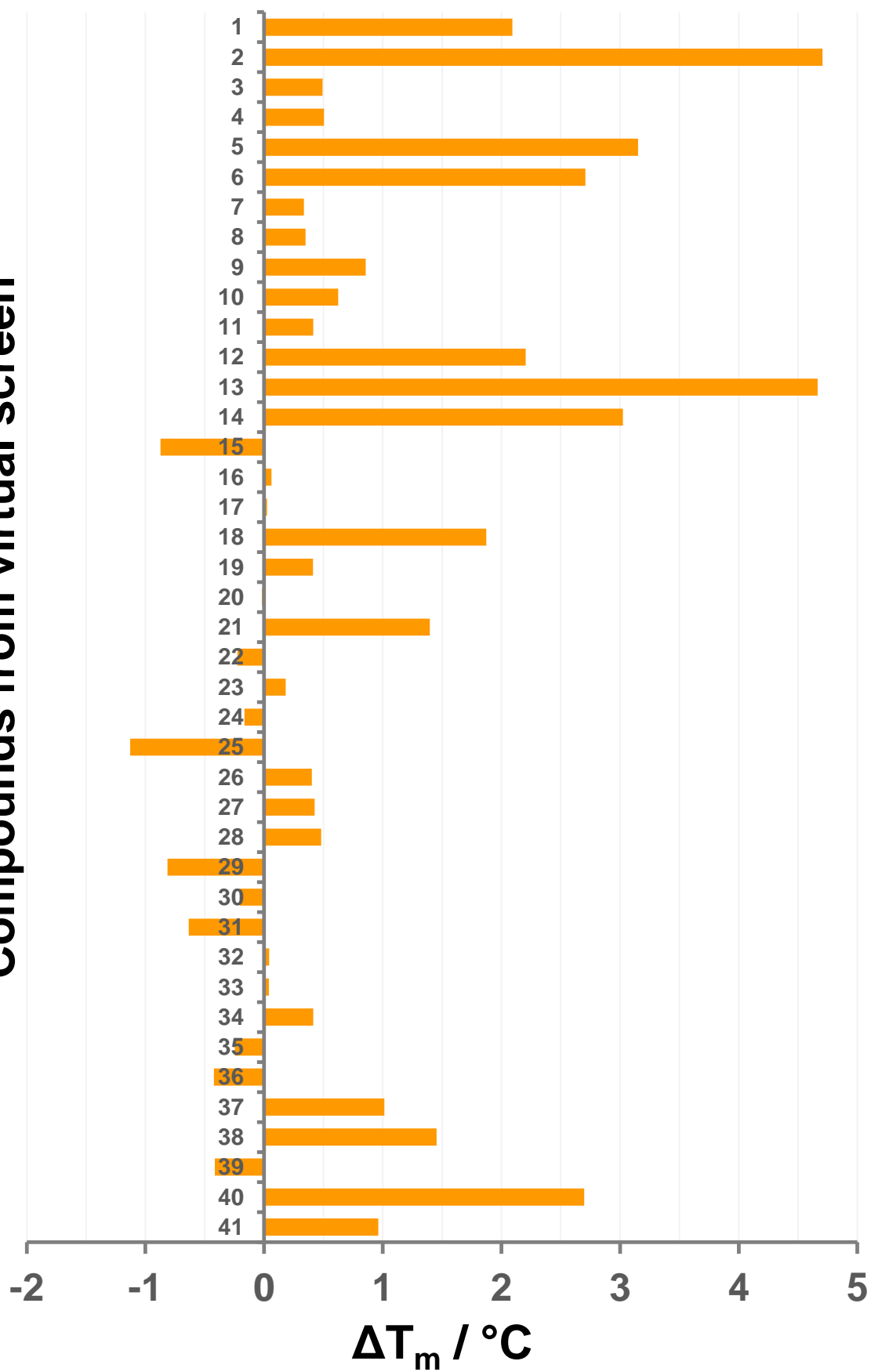


41

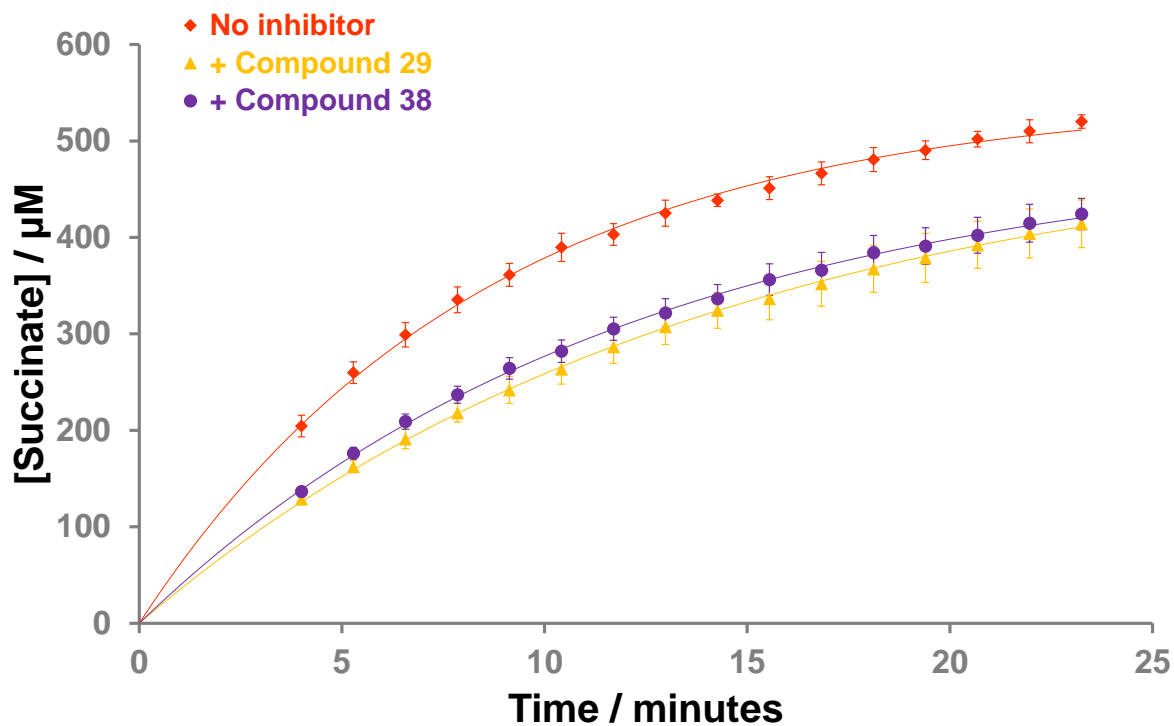


Supplementary Figure S12: Structures of the compounds obtained by virtual screening.

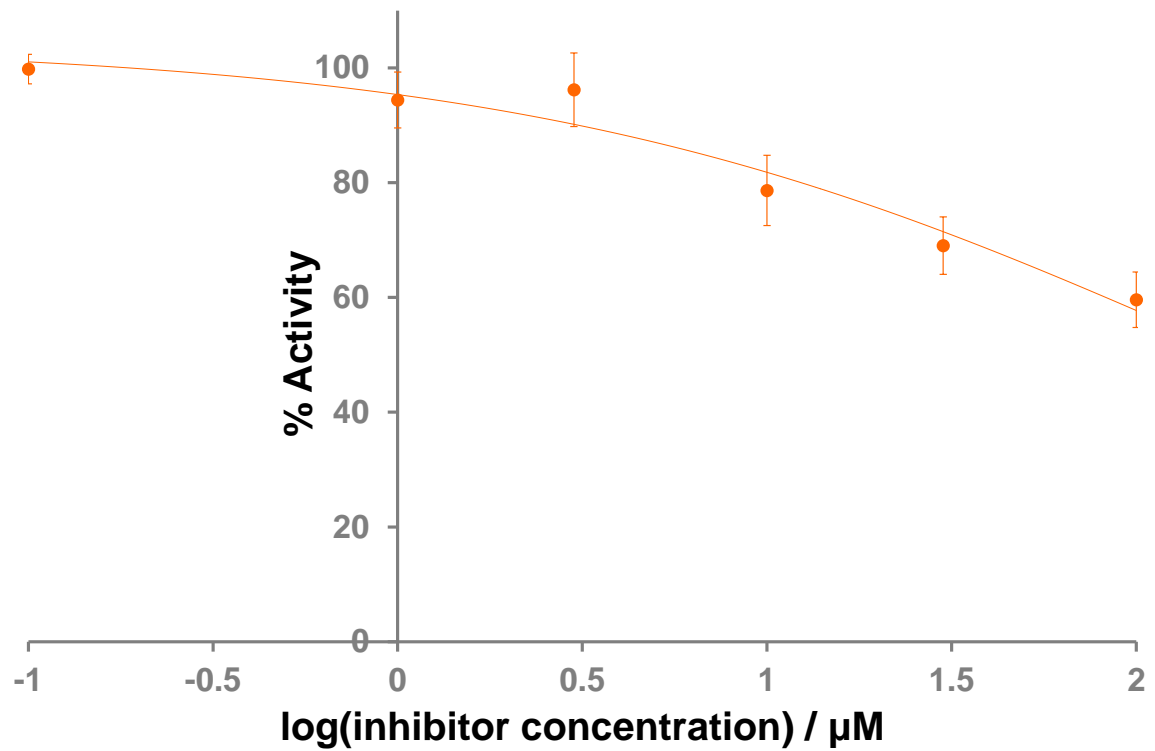
Compounds from virtual screen



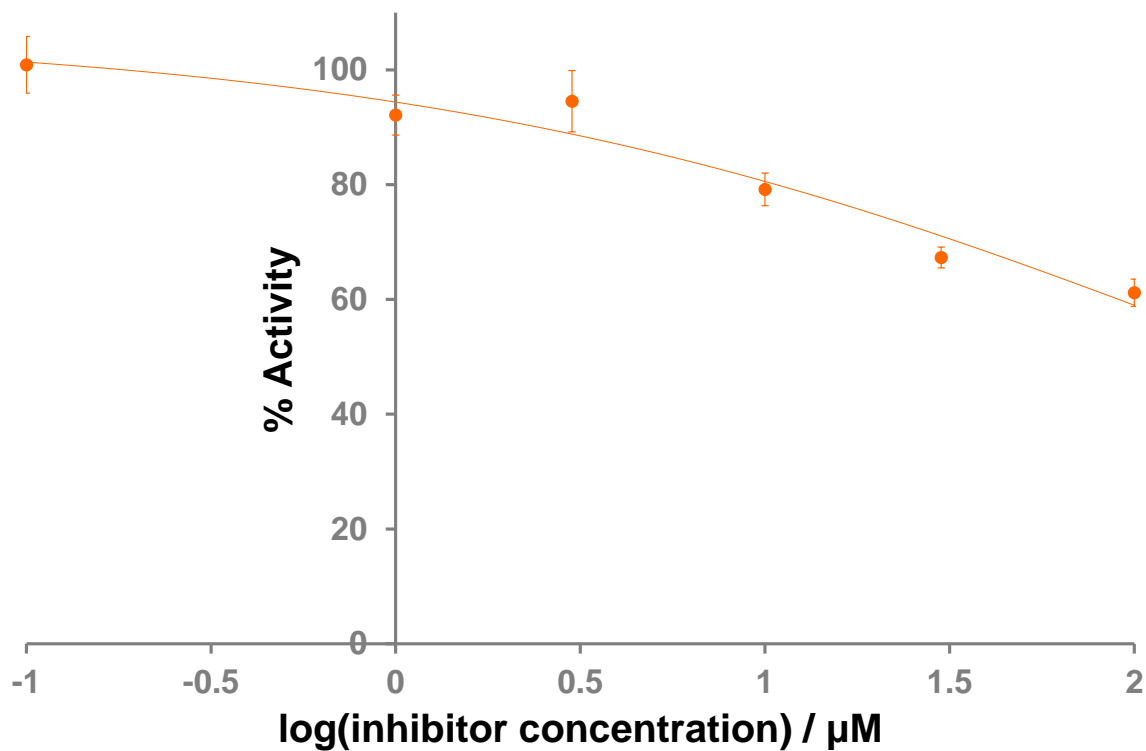
Supplementary Figure S13: Thermal shift data of ICL1 in the presence of compounds obtained from virtual screening. Sample contained 20 μ M ICL1, 1 mM compounds (where applicable) and 1 mM MgCl₂ in 50 mM Tris-HCl pH 7.5. Temperature was increased from 25 to 95 °C at 1 °C increment every 60 seconds. Compounds that gave a thermal shift (ΔT_m) of more than 0.5 °C were chosen for further testing by NMR. These included compounds **1, 2, 5, 6, 9, 10, 12, 13, 14, 15, 18, 21, 25, 29, 31, 37, 38, 40** and **41**.



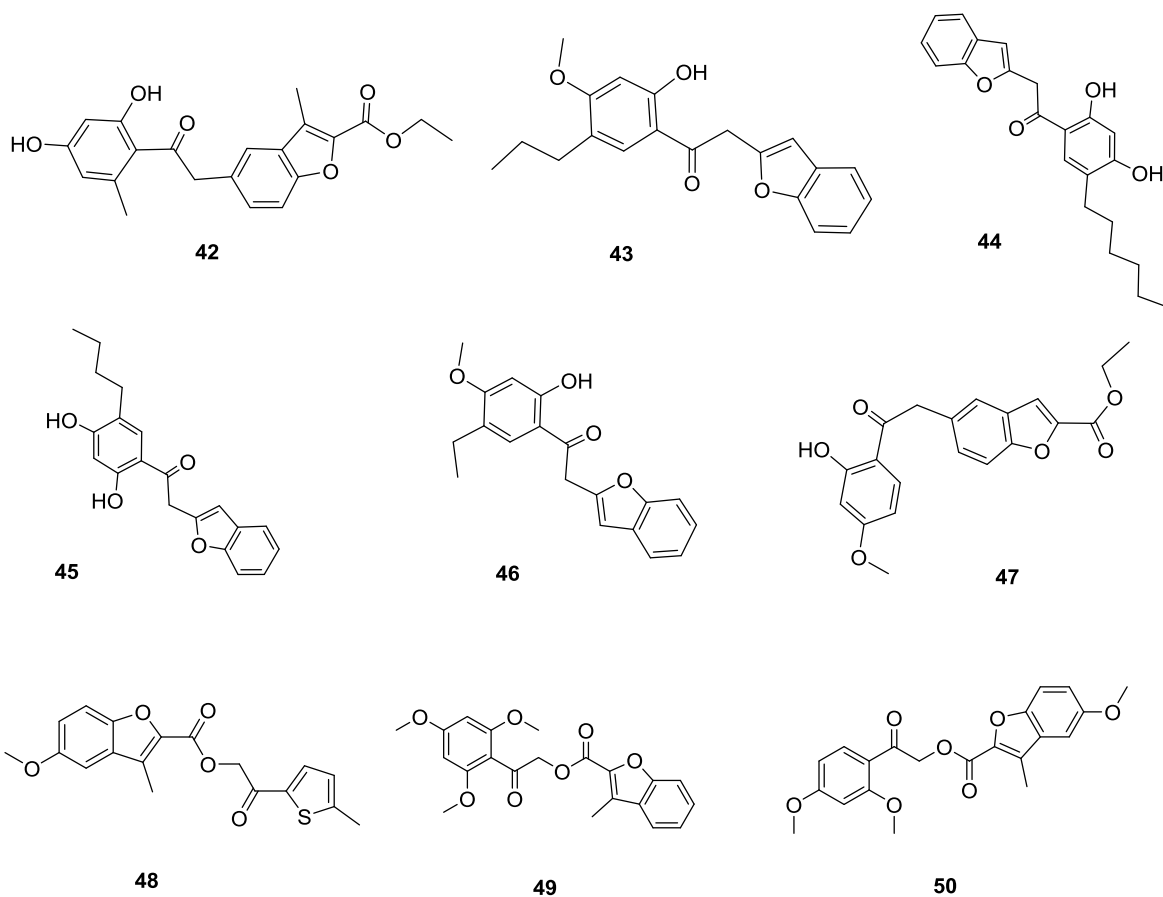
Supplementary Figure S14: Single concentration inhibition data of compounds **5** and **6** that were obtained by virtual screening. Sample contained 190 nM ICL1, 1 mM DL-isocitrate, 100 μM inhibitor (if applicable), 5 mM MgCl_2 and 50 mM Tris/Tris- D_{11} (pH 7.5) in 90% H_2O and 10% D_2O . The curves were added to aid visualisation. The errors shown are the standard deviation from three separate measurements.



Supplementary Figure S15: IC_{50} measurement for Compound **29**. Samples contained 190 nM ICL1, 1 mM DL-isocitrate, varying concentration of inhibitor, 5 mM MgCl_2 and 50 mM Tris/Tris- D_{11} (pH 7.5) in 90% H_2O and 10% D_2O . The errors shown are the standard deviation from three separate measurements. IC_{50} was $>100 \mu\text{M}$.



Supplementary Figure S16: IC₅₀ measurement for Compound **38**. Samples contained 190 nM ICL1, 1 mM DL-isocitrate, varying concentration of inhibitor, 5 mM MgCl₂ and 50 mM Tris/Tris-D₁₁ (pH 7.5) in 90% H₂O and 10% D₂O. The errors shown are the standard deviation from three separate measurements. IC₅₀ was >100 μM .



Supplementary Figure S17: Selected nine similar compounds (42-50) of identified hits 29 and 38.

| Compound | GS | CS | PLP | ASP |
|----------|------|------|------|------|
| 1 | 59.2 | 29.0 | 53.5 | 28.8 |
| 2 | 65.0 | 27.4 | 64.6 | 33.0 |
| 3 | 62.6 | 25.4 | 72.0 | 31.4 |
| 4 | 56.0 | 26.0 | 66.1 | 32.2 |
| 5 | 64.4 | 27.3 | 54.2 | 28.3 |
| 6 | 58.1 | 29.8 | 54.8 | 27.6 |
| 7 | 50.3 | 25.6 | 48.8 | 27.5 |
| 8 | 52.0 | 34.9 | 65.3 | 35.8 |
| 9 | 47.3 | 29.6 | 52.5 | 31.8 |
| 10 | 46.4 | 27.4 | 63.0 | 28.4 |
| 11 | 62.2 | 27.5 | 52.1 | 27.7 |
| 12 | 62.5 | 25.3 | 57.8 | 27.4 |

| | | | | |
|----|------|------|------|------|
| 13 | 52.3 | 25.8 | 49.7 | 28.2 |
| 14 | 54.5 | 27.8 | 59.3 | 31.6 |
| 15 | 53.6 | 28.8 | 53.2 | 25.9 |
| 16 | 55.4 | 31.5 | 54.5 | 29.0 |
| 17 | 56.4 | 28.0 | 54.1 | 26.8 |
| 18 | 56.0 | 30.9 | 63.6 | 31.4 |
| 19 | 71.1 | 27.5 | 66.6 | 29.7 |
| 20 | 61.3 | 28.1 | 65.7 | 32.3 |
| 21 | 54.4 | 28.9 | 59.5 | 26.9 |
| 22 | 65.4 | 32.0 | 69.0 | 32.1 |
| 23 | 64.4 | 34.0 | 63.3 | 30.6 |
| 24 | 66.6 | 31.9 | 64.5 | 32.5 |
| 25 | 65.2 | 27.4 | 55.2 | 31.1 |

| | | | | |
|----|------|------|------|------|
| 26 | 47.4 | 27.5 | 50.0 | 25.5 |
| 27 | 59.3 | 29.7 | 53.5 | 26.6 |
| 28 | 64.0 | 33.2 | 62.0 | 30.0 |
| 29 | 53.3 | 27.0 | 51.9 | 28.5 |
| 30 | 62.8 | 32.4 | 61.1 | 29.3 |
| 31 | 55.6 | 31.6 | 58.6 | 30.0 |
| 32 | 62.9 | 25.5 | 49.3 | 26.7 |
| 33 | 63.0 | 27.0 | 59.4 | 27.9 |
| 34 | 62.9 | 31.5 | 62.4 | 30.5 |
| 35 | 63.0 | 31.4 | 59.2 | 30.1 |
| 36 | 57.6 | 30.8 | 59.0 | 27.3 |
| 37 | 55.9 | 28.0 | 51.2 | 25.7 |
| 38 | 51.1 | 31.6 | 65.0 | 28.2 |

| | | | | |
|----|------|------|------|------|
| 39 | 62.6 | 26.0 | 64.8 | 32.7 |
| 40 | 55.4 | 27.4 | 70.0 | 27.9 |
| 41 | 49.4 | 29.3 | 55.2 | 30.0 |
| 42 | 40.8 | 27.1 | 38.0 | 19.5 |
| 43 | 51.8 | 31.0 | 53.1 | 25.7 |
| 44 | 55.4 | 31.0 | 62.0 | 25.0 |
| 45 | 52.4 | 28.5 | 43.7 | 26.4 |
| 46 | 50.1 | 27.5 | 48.2 | 23.5 |
| 47 | 52.2 | 26.2 | 49.5 | 26.2 |
| 48 | 52.5 | 23.5 | 33.3 | 17.3 |
| 49 | 58.3 | 25.7 | 52.9 | 24.5 |
| 50 | 42.9 | 21.5 | 40.7 | 23.2 |

Supplementary Table S1: Scoring results of the 41 virtual hits.

| Compound | MW | HB Donor | HB Acceptor | Log P | PSA | Rot. bonds |
|----------|-------|----------|-------------|-------|-------|------------|
| 1 | 443.5 | 2.5 | 8.0 | 4.0 | 149.9 | 9 |
| 2 | 401.4 | 1.0 | 7.0 | 3.3 | 138.9 | 11 |
| 3 | 415.4 | 1.0 | 7.0 | 3.4 | 138.5 | 12 |
| 4 | 415.4 | 1.0 | 7.0 | 3.6 | 139.7 | 12 |
| 5 | 358.3 | 1.0 | 6.0 | 3.2 | 113.5 | 7 |
| 6 | 283.3 | 4.0 | 4.0 | 1.3 | 82.5 | 6 |
| 7 | 373.4 | 0.0 | 7.0 | 3.2 | 81.8 | 4 |
| 8 | 464.5 | 0.0 | 8.0 | 3.5 | 119.7 | 4 |
| 9 | 413.5 | 2.0 | 8.0 | 2.8 | 125.9 | 6 |
| 10 | 166.2 | 2.0 | 3.5 | -1.5 | 85.2 | 4 |
| 11 | 340.3 | 0.0 | 6.0 | 3.0 | 83.3 | 4 |

| | | | | | | |
|----|-------|-----|-----|-----|-------|----|
| 12 | 286.2 | 1.0 | 6.0 | 1.9 | 106.1 | 4 |
| 13 | 301.3 | 2.0 | 5.0 | 2.5 | 109.4 | 6 |
| 14 | 342.3 | 4.0 | 9.0 | 0.8 | 183.3 | 7 |
| 15 | 270.3 | 0.0 | 4.5 | 2.3 | 75.6 | 6 |
| 16 | 284.3 | 0.0 | 4.5 | 2.7 | 75.6 | 6 |
| 17 | 300.3 | 0.0 | 5.0 | 2.4 | 83.2 | 7 |
| 18 | 230.2 | 0.0 | 4.0 | 1.7 | 78.4 | 5 |
| 19 | 421.4 | 3.5 | 7.0 | 1.6 | 123.9 | 12 |
| 20 | 276.2 | 1.0 | 5.0 | 1.3 | 113.9 | 6 |
| 21 | 323.1 | 1.0 | 3.0 | 2.8 | 73.7 | 6 |
| 22 | 288.3 | 1.0 | 4.0 | 3.1 | 81.9 | 8 |
| 23 | 258.6 | 1.0 | 3.0 | 2.8 | 75.1 | 6 |
| 24 | 286.3 | 1.0 | 3.0 | 3.3 | 74.8 | 7 |

| | | | | | | |
|----|-------|-----|-----|-----|-------|---|
| 25 | 290.3 | 1.0 | 4.0 | 2.5 | 100.2 | 8 |
| 26 | 165.2 | 0.0 | 4.0 | 1.2 | 56.9 | 4 |
| 27 | 288.2 | 1.0 | 4.0 | 3.1 | 76.2 | 7 |
| 28 | 268.3 | 1.0 | 3.0 | 2.8 | 74.3 | 5 |
| 29 | 328.3 | 1.0 | 6.0 | 2.8 | 99.7 | 6 |
| 30 | 340.3 | 1.0 | 5.0 | 2.7 | 113.1 | 7 |
| 31 | 279.3 | 1.0 | 3.5 | 2.8 | 77.8 | 5 |
| 32 | 318.3 | 1.0 | 5.0 | 2.7 | 108.8 | 8 |
| 33 | 219.2 | 1.0 | 4.0 | 1.1 | 88.2 | 5 |
| 34 | 229.2 | 1.0 | 3.5 | 2.0 | 73.0 | 5 |
| 35 | 302.3 | 2.0 | 5.0 | 1.9 | 99.7 | 6 |
| 36 | 286.3 | 1.0 | 4.0 | 2.5 | 80.5 | 5 |
| 37 | 310.3 | 1.0 | 3.0 | 3.9 | 72.6 | 7 |

| | | | | | | |
|----|-------|-----|-----|------|-------|----|
| 38 | 354.4 | 1.0 | 5.0 | 3.3 | 108.7 | 7 |
| 39 | 439.4 | 2.0 | 9.0 | 2.2 | 177.5 | 9 |
| 40 | 494.5 | 3.0 | 7.0 | 3.4 | 151.9 | 11 |
| 41 | 182.2 | 5.5 | 5.5 | -1.0 | 89.1 | 7 |
| 42 | 348.2 | 0.0 | 9.0 | 0.5 | 134.6 | 5 |
| 43 | 304.2 | 0.0 | 5.0 | 2.7 | 71.7 | 5 |
| 44 | 328.2 | 0.0 | 6.5 | 2.3 | 94.2 | 4 |
| 45 | 304.2 | 0.0 | 6.5 | 1.6 | 95.4 | 4 |
| 46 | 292.2 | 0.0 | 5.0 | 2.4 | 70.0 | 5 |
| 47 | 336.2 | 0.0 | 7.5 | 1.0 | 118.3 | 6 |
| 48 | 328.3 | 0.0 | 5.5 | 2.5 | 85.5 | 5 |
| 49 | 364.2 | 0.0 | 6.5 | 2.5 | 96.3 | 7 |
| 50 | 364.2 | 0.0 | 6.5 | 2.5 | 102.2 | 7 |

Supplementary Table S2: The calculated molecular descriptors for the identified virtual hits (1-41) and their structural derivatives.

Protein sequence:

MSVVGTPKSA EQIQQEWDTN PRWKDVTRTY SAEDVVALQG SVVEEHTLAR RGAEVLWEQL
HDLEWVNALG ALTGNMAVQQ VRAGLKAIYL SGWQVAGDAN LSGHTYPDQS LYPANSVPQV
VRRINNALQR ADQIAKIEGD TSVENWLAPI VADGEAGFGG ALNVYELQKA LIAAGVAGSH
WEDQLASEKK CGHLGGKVL I PTQQHIRT LT SARLAADVAD VPTVVIARTD AEAATLITSD
VDERDQPFIT GERTREGFYR TKNGLIEPCIA RAKAYAPFAD LIWMETGTPD LEAARQFSEA
VKA EY PDQML AYNCS P S F NW K KHLDDATIA KFQKEL AAMG FKFQFITLAG FHALNYSMFD
LAYGYAQNQM SAYVELQERE FAAEERGYTA TKHQREVGAG YFDRIATTVD PNSSTTALTG
STEEGQFH

Synthetic gene design:

tacttccaatcc
atgtctgtcg tcggcacccc gaagagcgcg gagcagatcc agcaggaatg ggacacgaac
ccgcgctgga aggacgtcac ccgcacctac tccgccgagg acgtcgtcgc cctccagggc
agcgtggteg aggagcacac gctggccccg cgcggtgcgg aggtgctgtg ggagcagctg
cacgacctcg agtgggtcaa cgcgctgggc gcgctgaccg gcaacatggc cgtccagcag
gtgcgcgccg gcctgaaggc catctacctg tcgggctggc aggtcgccgg cgatgccaac
ctgtccgggc acacctacc caccagagc ctgtatcccg ccaactcggg gccgcaggtg
gtccgccgga tcaacaacgc actgcagcgc gccgaccaga tcgcccaagat cgagggcgat
acttcggtgg agaactggct ggcgccgatt gtcgccgacg gcgaggccgg ctttggcggc
gcgctcaacg tctacgagct gcagaaagcc ctgatcgccg cgggcggtgc gggttcgcac
tgggaggacc agttggcctc tgagaagaag tgcggccacc tgggcggcaa ggtgttgatc
ccgaccagc agcacatccg cactttgacg tctgctcggc tcgcggccga tgtggctgat
gttcccacgg tggatgatcg ccgtaccgac gccgaggcgg ccacgctgat cacctccgac
gtcgacgagc gcgaccagcc gttcatcacc ggcgagcgca cccgggaagg cttctaccgc
accaagaacg gcatcgagcc ttgcatcgct cgggcgaagg cctacgccc gttcgcgac
ttgatctgga tggagaccgg taccocggac ctcgaggccg cccggcagtt ctccgaggcg
gtcaaggcgg agtaccgga ccagatgctg gcctacaact gctcgccatc gttcaactgg
aaaaagcacc tcgacgagc caccatcgcc aagttccaga aggagctggc agccatgggc
ttcaagttcc agttcatcac gctggccggc ttccatgcgc tgaactactc gatgttcgat
ctggcctacg gctacgccc gaaccagatg agcgcgtatg tcgaactgca ggaacgcgag
ttcgccgccc aagaacgggg ctacaccgcg accaagcacc agcgcgaggt cggcgccggc
tacttcgacc ggattgccac caccgtggac ccgaattcgt cgaccaccgc gttgaccggt
tccaccgaag agggccagtt ccactag
cagtaaaggtggata

Supplementary Table S3: Sequence of ICL1 and the synthetic gene fragment used in this study.

Sequences *tacttccaatcc* and *cagtaaaggtggata* were added to the 5' and 3' ends respectively for cloning to the vector pNIC28-Bsa4 (See Materials and Methods).